

An assessment of progressive damage in mechanical joint of GLASS/EPOXY composite under quasi-static loading

Nabi Mehri Khansari^{a*} and Mehdi Sepehrifar^a

^aFaculty of Mechanical Engineering, Sahand University of Technology, Tabriz, Iran

ARTICLE INFO

Article history:

Received 18 August 2025

Accepted 12 November 2025

Available online

12 November 2025

Keywords:

Fracture Mechanics

Thermoplastic Composites

Quasi-static loading

Progressive Damage

ABSTRACT

The prediction of crack initiation and propagation of damage initiation and propagation in composite structures has gained significant attention due to the increasing use of these materials in the aerospace industry. In this context, estimating progressive damage in composite ply is crucial, as it refers to the gradual failure and deformation of the structure, which can lead to a reduction in the useful life and safety of the structure. By examining these damages, it is possible to identify the causes and factors contributing to their occurrence and to propose suitable solutions for preventing and repairing the damages. In the present study, an effort is made to develop numerical, analytical, and experimental approaches for modeling and estimating progressive damage at mechanical joints in composite aircraft structures, considering quasi-static loading, including tensile loading. The study incorporates an investigation of damage mechanisms such as fiber breakage, matrix cracking, and delamination that commonly occur in composite laminates under mechanical stress. Combining modeling and experimental results allows for a comprehensive understanding of damage evolution, enabling the formulation of strategies aimed at improving the durability and safety of composite structures in aerospace applications. Ultimately, based on the results of modeling and experiments, strategies will be proposed to enhance the lifespan of the structure.

© 2026 Growing Science Ltd. All rights reserved.

1. Introduction

Modeling damage mechanisms in polymer composite materials remains a central research topic due to its critical importance for aerospace structural reliability. The initial progressive damage model for laminate composites under tensile loading was introduced by Chang & Chang, (1987) effectively predicting strength reduction. Experimental validations by Harris et al. (1997) confirmed the model's accuracy in capturing damage progression and stiffness loss in aircraft structures. Finite element simulations were done (Papanikos et al., 2003; Roy & Srivastav, 2017) successfully to predict the damage initiation and evolution in unidirectional composites. The structural efficacy of glass/epoxy composites in load-bearing applications is critically contingent upon the integrity of their mechanically fastened joints. While substantial research has been dedicated to predicting the ultimate failure strength of such joints under quasi-static conditions using established standards and models (Christensen, 1997; Dano et al., 2000), their performance under recurrent operational loads—a scenario endemic to aerospace, automotive, and renewable energy structures—presents a more complex challenge. The prevailing literature has extensively cataloged failure modes such as bearing failure and net-tension, often through the lens of static failure criteria and two-dimensional stress analysis (Dano et al., 2000; Echaabi et al., 1996; Li, 2020). However, this paradigm offers limited insight into the gradual, cumulative damage processes that govern joint integrity long before catastrophic failure manifests. The transition from a pristine state to final rupture is not a discrete event but a continuum of material state evolution, the mechanics of which remain inadequately quantified for glass/epoxy systems under quasi-static loading, particularly when compared to the advanced multi-scale and probabilistic approaches being developed for other composite systems (Bogdanovich, 2009; Ghosh et al., 2025; Khansari et al., 2019). This damage continuum is characterized by an irreversible energy dissipation mechanism that conventional static models fail to capture. Initial damage in the form of matrix micro-

* Corresponding author.

E-mail addresses: n.mehri@sut.ac.ir (N. M. Khansari)

ISSN 2291-8752 (Online) - ISSN 2291-8744 (Print)

© 2026 Growing Science Ltd. All rights reserved.

doi: 10.5267/j.esm.2025.11.003

cracking and interfacial debonding at the bolt-hole contact region alters the local stiffness and creates internal friction, a process that micromechanical analyses have shown to be a precursor to macroscopic failure (Kaleel et al., 2018; Mehri Khansari et al., 2022; Sun et al., 2019). Under quasi-static loading, this manifests as a progressive evolution in the joint's hysteresis behavior—the lag between applied load and resultant displacement. The shape, area, and drift of the hysteresis loop serve as a direct, macroscopic signature of the underlying damage accumulation. The enlargement of the hysteresis area signifies increased energy dissipation through frictional sliding between fracture surfaces and viscoelastic damping in the damaged epoxy matrix, while a drift in the loop indicates permanent deformation and stiffness loss. Current progressive damage models, often focused on ultimate strength prediction for complex architectures like 3D woven or braided composites (Bogdanovich, 2009; Zhang et al., 2015; Zheng et al., 2022) or impact scenarios (Cutting, 2025; Shokrieh & Omid, 2010), typically overlook this critical hysteretic energy metric as a primary diagnostic for damage state in bolted joints. This framework allows for the delineation of distinct damage phases: an initial phase of hysteresis stabilization, a subsequent phase of steady, cumulative energy dissipation, and a terminal phase of rapid hysteresis growth preceding ultimate failure. This data-driven approach to damage characterization aligns with the emerging paradigm of using measurable operational data to inform material state awareness, a concept explored in machine learning-based diagnosis (Mehri Khansari et al., 2024; Shamsirband & Mehri Khansari, 2021) but not yet fully leveraged for mechanical joint analysis. To validate this framework, an experimental investigation was conducted on single-bolt, double-shear glass/epoxy composite joints subjected to tension-tension quasi-static loading. The load-displacement hysteresis loops were meticulously recorded and analyzed to extract energy dissipation metrics. These experimental observations are complemented by a finite element model that incorporates a cohesive zone formulation, informed by mixed-mode fracture investigations (Mehri Khansari & Aliha, 2023; Papanikos et al., 2003; Roy & Srivastav, 2017), to simulate interlaminar damage and a contact model with friction to capture the energy dissipation mechanisms at the micro-crack interfaces. The objective is to establish a direct correlation between the experimentally measured strength and the simulated internal damage state, thereby proposing a novel methodology for predicting the progressive damage and assessing the damage tolerance of mechanically fastened glass/epoxy composites under quasi-static service conditions, bridging a gap between traditional mechanical testing and modern prognostic modeling techniques (Ghosh et al., 2025; Gljušćić et al., 2022; Talreja, 2006). The structural integrity of mechanically fastened joints in polymer-based composites is paramount to the safety and performance of modern engineering systems. Predicting failure in these regions remains a formidable challenge due to the complex interplay of stress concentrations, material anisotropy, and progressive damage mechanisms (Dano et al., 2000; Talreja, 2006). While the development of failure criteria has a long and rich history, from foundational works to contemporary refinements (Christensen, 1997; Echaabi et al., 1996; Hashin, 1980), many existing modeling approaches exhibit a critical limitation: a reliance on a single failure theory to describe a multi-modal damage process (Kodagali, 2017; Li, 2020). This can lead to inaccurate predictions, as different failure modes—such as matrix crushing in bearing; shear-out, and net-tension fracture—are governed by distinct mechanical drivers and may be best captured by different theoretical models. This study introduces a comprehensive, multi-criteria integrated framework to overcome this limitation. Unlike previous works that often focus on a single failure criterion or isolated loading conditions, the present approach synergistically combines analytical and numerical methodologies, leveraging experimentally obtained mechanical properties as a foundational input, consistent with standardized testing protocols (ASTM- D3039, 2008). The framework's core innovation lies in the concurrent implementation of multiple, established failure criteria—including HASHIN (Hashin, 1980; Hashin & Rotem, 1973), Hoffman, Puck (Echaabi et al., 1996), maximum stress, and maximum strain (Li, 2020)—within a unified progressive damage algorithm. This multi-faceted lens allows the model to dynamically select the most appropriate failure initiation mechanism for each constituent (fiber and matrix) and at each material point, based on the local stress state. This is a significant departure from methodologies that force a complex, multi-axial stress field to conform to a single, potentially non-optimal, failure envelope, a simplification common in earlier progressive damage studies (Bogdanovich, 2009; Lin et al., 2021). The integration of this multi-criteria damage model within a robust numerical finite element framework enables high-fidelity simulation of the entire damage evolution process, building upon advanced techniques used in multiscale (Ghosh et al., 2025; Kaleel et al., 2018) and meso-scale (Zhang et al., 2015; Zheng et al., 2022) modeling. The model sequentially accounts for the initiation of damage, its propagation based on energy-based degradation laws, and the consequent redistribution of stresses, leading to the final failure of the joint. By systematically comparing the predictions of each criterion and their amalgamated result against experimental data from instrumented bolted-joint tests, this work aims to identify not only the most accurate failure load prediction but also to elucidate the specific strengths and weaknesses of each criterion at different stages of the damage trajectory. The outcome is a validated, high-fidelity simulation tool that provides a more nuanced and reliable prediction of damage evolution in jointed composite structures, offering significant value for the design and certification of composite-intensive assemblies. Furthermore, the coupling of experimental data with advanced numerical simulations enables validation and refinement of damage models under realistic service conditions, setting this study apart from models relying solely on theoretical or simplified assumptions.

2. Theoretical Concepts

Progressive damage analysis in composite materials involves identifying the failure of each individual ply under applied loading. To begin this process, the stress state across the entire laminate must be determined. Once the stress distribution is known, an appropriate failure criterion is applied to assess damage in the most critical ply. This allows identifying which ply fails at which load level. The procedure continues interactively until the failure of the final ply is established. After applying boundary conditions and defining damage parameters, the analysis software evaluates the selected failure criteria for each ply.

Based on the stress state, the sequence of ply failures is determined. Various failure criteria are used to identify damage in composites, which can be broadly categorized into stress-based and strain-based approaches. In stress-based criteria, experimental measurements do not directly influence the damage prediction process, whereas in strain-based criteria, experimental strain values play a direct role in the progression of damage. Therefore, both types of criteria are employed in this study to ensure a comprehensive evaluation. Failure criteria can also be classified into interactive and non-interactive types. Interactive criteria consider the coupling effects between stress and strain components, while non-interactive criteria treat each component independently. Additionally, some failure criteria are capable of identifying the specific failure mode (e.g., fiber breakage, matrix cracking), whereas others only indicate the occurrence of failure without distinguishing its nature (Hashin, 1980; Tsai & Wu, 1971). In the following sections, several relevant failure criteria used to identify the initial failure in composite laminates are examined and discussed. The Maximum Stress Criterion is one of the earliest methods introduced for evaluating failure in composites. According to this criterion, failure does not occur if the magnitude of each stress component along the principal material directions is less than the corresponding strength in that direction. Based on this, the criterion for tensile stresses is expressed by following equation (Tsai & Wu, 1971).

$$\frac{\sigma_x}{X_T} = 1, \frac{\sigma_y}{Y_T} = 1 \quad (1)$$

In the above relation, X_T and Y_T represent the tensile strengths in the fiber direction and transverse to the fiber direction, respectively (Eq. (1)) (Tsai & Wu, 1971). The Maximum Strain Criterion is very similar to the Maximum Stress Criterion, with the key difference that it uses strain components instead of stress components. According to this criterion, failure does not occur if the magnitude of each strain component along the principal material directions is less than the corresponding strain strength in that direction. Therefore, this criterion for tensile strains is defined by the equation.

$$\frac{\epsilon_x}{\epsilon_{XT}} = 1, \frac{\epsilon_y}{\epsilon_{YT}} = 1 \quad (2)$$

In the Eq. (2) relation, ϵ_{YT} and ϵ_{XT} represent the maximum allowable tensile strain in the fiber direction and transverse to the fiber direction, respectively. Also, Hoffman used Hill's equation to calculate different tensile and compressive strengths and proposed the following relation for the failure of composites.

$$C_2(\sigma_z - \sigma_x)^2 + C_3(\sigma_x - \sigma_y)^2 + C_4\sigma_x + C_5\sigma_y + C_6\sigma_z + C_7\tau_{yz}^2 + C_8\tau_{zx}^2 + C_9\tau_{xy}^2 = 1 \quad (3)$$

In the above relation, the 9 coefficients C_i are calculated based on 9 strengths in the principal directions $S_{23}, S_{31}, S_{12}, Z_C, Z_T, Y_C, Y_T, X_C, X_T$. In the two-dimensional case, where $\sigma_3 = \tau_{31} = \tau_{23} = 0$, and the transverse strengths are equal ($Y_T = Z_T, Y_C = Z_C, S_{12} = S_{31}$), Hoffman's criterion in two dimensions can be expressed as follows.

$$-\frac{\sigma_x^2}{X_T X_C} + \frac{\sigma_x \sigma_y}{X_T X_C} - \frac{\sigma_y^2}{Y_T Y_C} + \left(\frac{X_T + X_C}{X_T X_C}\right)\sigma_x + \left(\frac{Y_T + Y_C}{Y_T Y_C}\right)\sigma_y + \left(\frac{\tau_{xy}}{S}\right)^2 = 1 \quad (4)$$

As observed in the above relations, this criterion considers the interaction between stress and strain components, but it lacks the capability to assess the failure mode. To improve the accuracy of failure prediction, HASHIN (Echaabi et al., 1996) divided his model into four parts, including fiber tension and compression failure and matrix tension and compression failure. In this criterion, the fiber tensile failure is influenced not only by axial tensile stresses but also by shear stresses. This criterion is mathematically formulated, and its value is defined as follows.

$$\left(\frac{\sigma_x}{X_T}\right)^2 + \left(\frac{\tau_{xy}}{S}\right)^2 = 1 \quad (5)$$

The fiber compressive failure in HASHIN's criterion is defined by following equation.

$$\left(\frac{\sigma_x}{X_C}\right)^2 = 1 \quad (6)$$

Regarding matrix tensile failure, HASHIN's criterion provides a specific equation to define it, analogous to other failure modes in the composite. This part of the criterion addresses failure due to tensile stresses in the matrix material distinct from fiber failure modes.

$$\left(\frac{\sigma_y}{Y_T}\right)^2 + \left(\frac{\tau_{xy}}{S}\right)^2 = 1 \quad (7)$$

As observed in the above relations, this criterion considers the interaction between stress and strain components and also has the capability to evaluate the failure mode. PUCK's criterion divides the failure mechanism into two parts: fiber failure and matrix failure, examining each independently. According to this criterion, once fiber failure occurs, the composite ply can no longer carry load. However, matrix failure does not necessarily imply fiber fracture, so the fibers may continue to carry the load. The relations for fiber failure under tensile and compressive conditions are defined by the following equations.

$$\frac{\sigma_x}{X_T} = 1, -\frac{\sigma_y}{Y_T} = 1 \quad (8)$$

The relations of this criterion for matrix failure due to normal and shear stresses are defined by equation.

$$\frac{\sigma_y^2}{Y_T Y_C} + \frac{\tau_{xy}^2}{S^2} + \left(\frac{1}{Y_T} + \frac{1}{Y_C}\right)\sigma_y = 1 \quad (9)$$

As observed in the above relations, this criterion takes into account the interaction between stress and strain components and also has the capability to identify the failure mode. The biaxial failure criterion requires some modifications through testing. Sai-Wu proposed a method that includes a new definition of strength between stresses. The Sai-Wu criterion in three dimensions consists of six stress components, which are:

$$F_{\alpha\beta}\sigma_{\alpha\beta} + F_{\alpha\beta\gamma\delta}\sigma_{\alpha\beta}\sigma_{\gamma\delta} + \dots = 1 \quad (10)$$

In this relation F_α , $F_{\alpha\beta}$ are strength tensors of various orders. Eq. (11) for the plane stress condition with membrane stresses is expressed as follows.

$$F_1\sigma_1 + F_2\sigma_2 + F_{11}\sigma_1^2 + 2F_{12}\sigma_1\sigma_2 + F_{22}\sigma_2^2 + F_{66}\sigma_6^2 = 1 \quad (11)$$

To calculate the values of the strength tensors, as in previous methods, the relations are evaluated separately. Therefore, in the 1th step, the specimen is subjected to independent tensile stress, and Eq. (12) is simplified as follows:

$$F_1 X_t + F_{11} F_t^2 = 1 \quad (12)$$

By simultaneously solving Eq. (12) and Eq. (10), the following relation is obtained:

$$F_1 = \frac{1}{X_T} - \frac{1}{X_C}; \quad F_{11} = -\frac{1}{X_T X_C} \quad (13)$$

also,

$$F_2 = \frac{1}{Y_T} - \frac{1}{Y_C}; \quad F_{22} = -\frac{1}{Y_T Y_C} \quad (14)$$

By applying the shear stress τ_{12} and considering its sign, the result is:

$$F_6 = 0; \quad F_{22} = -\frac{1}{S^2} \quad (15)$$

Hill proposed the following criterion for the yield of orthotropic materials.

$$(G+H)\sigma_1^2 + (F+H)\sigma_2^2 + (F+G)\sigma_3^2 - 2H\sigma_1\sigma_2 - 2H\sigma_1\sigma_3 - 2F\sigma_2\sigma_3 + 2L\tau_{23}^2 + 2M\tau_{13}^2 + 2N\tau_{12}^2 = 1 \quad (16)$$

Hill's yield stresses including F, G, H, L, M and N , assuming linear elastic behavior, can be considered as failure strengths. The Hill criterion is derived using the von Mises criterion. Sai calculated the failure parameters of Eq. (11) based on failure strengths and S for a single ply. If only shear stress τ_{12} is applied on the body, since the maximum of this stress equals (S), the following result is obtained:

$$2N = \frac{1}{S^2} \tag{17}$$

By applying σ_1 :

$$G + H = \frac{1}{X^2} \tag{18}$$

If the σ_2 is applied:

$$F + H = \frac{1}{Y^2} \tag{19}$$

Eventually if the σ_3 is applied:

$$F + G = \frac{1}{Z^2} \tag{20}$$

Z is the strength of the ply in the direction of the 3-axis. The above coefficients can be calculated based on the strengths.

$$\begin{aligned} 2F &= \frac{1}{Y^2} + \frac{1}{Z^2} - \frac{1}{X^2} \\ 2G &= \frac{1}{X^2} + \frac{1}{Z^2} - \frac{1}{Y^2} \\ 2H &= \frac{1}{X^2} + \frac{1}{Y^2} - \frac{1}{Z^2} \end{aligned} \tag{21}$$

For plane stresses in the plane and for a unidirectional single ply, the values can be simplified.

$$\sigma_3 = \tau_{13} = \tau_{23} = 0 \tag{22}$$

It is also assumed that the strength in the 3-direction is equal, and consequently, $Z=Y$. Finally, the Sai-Hill failure criterion in the plane is expressed as follows.

$$\frac{\sigma_1^2}{X^2} - \frac{\sigma_1\sigma_2}{X^2} + \frac{\sigma_2^2}{Y^2} + \frac{\tau_{12}^2}{S^2} = 1 \tag{23}$$

This study employs both analytical and numerical techniques to forecast damage in jointed composite materials following the acquisition of experimental data and mechanical properties. Various failure criteria, including those by HASHIN, Hoffman, PUCK, as well as maximum stress and maximum strain criteria are utilized to evaluate the damage prediction in the jointed composites. Damage growth modeling is discussed in cases where a specific damage evolution model is defined. Prior to the initiation of damage, the material behaves as a linearly elastic medium, and its stiffness matrix corresponds to the plane stress condition of an orthotropic material. In a Cartesian coordinate system aligned with the principal orthotropic directions, the constitutive relations of the material are expressed as follows.

$$\boldsymbol{\varepsilon}_i = \mathbf{C}_{ij} \boldsymbol{\sigma}_j \tag{24}$$

The constants C'_{ij} in the Eq. (24) are obtained from the constitutive equation that is defined as follows:

$$\begin{pmatrix} \varepsilon_{11} \\ \varepsilon_{22} \\ \varepsilon_{33} \\ \gamma_{23} \\ \gamma_{31} \\ \gamma_{12} \end{pmatrix} = \begin{pmatrix} 1/E_1 & -\nu_{21}/E_2 & -\nu_{31}/E_3 & 0 & 0 & 0 \\ -\nu_{12}/E_1 & 1/E_2 & -\nu_{32}/E_3 & 0 & 0 & 0 \\ -\nu_{13}/E_1 & -\nu_{23}/E_2 & 1/E_3 & 0 & 0 & 0 \\ 0 & 0 & 0 & 1/G_{23} & 0 & 0 \\ 0 & 0 & 0 & 0 & 1/G_{31} & 0 \\ 0 & 0 & 0 & 0 & 0 & 1/G_{12} \end{pmatrix} \begin{pmatrix} \sigma_{11} \\ \sigma_{22} \\ \sigma_{33} \\ \sigma_{23} \\ \sigma_{31} \\ \sigma_{12} \end{pmatrix} \tag{25}$$

For the plane stress condition in the (x_1, x_2) plane, only the components $C_{11}, C_{22}, C_{12}, C_{21}$ and C_{66} remain active. Furthermore, for plane strain problems, the governing equations are identical to those of the plane stress condition, except for four components of the stiffness matrix, which differ and are defined by the modified matrix C'_{ij} as follows:

$$C'_{ij} = C_{ij} - C_{i3}C_{j3} / C_{33} \quad (i, j = 1, 2) \tag{26}$$

for an isotropic based material including reinforcement, the following relationship is considered to satisfy the equilibrium condition of the matrix stresses when damage is exist.

$$\sigma = C_d \varepsilon \quad (27)$$

in which, C_d is damage stiffness matrix that is defined as Eq. (28)

$$C_d = \frac{1}{D} \begin{bmatrix} (1-d_f)E_1 & (1-d_f)(1-d_m)v_{21}E_1 & 0 \\ (1-d_f)(1-d_m)v_{12}E_2 & (1-d_m)E_2 & 0 \\ 0 & 0 & GD(1-d_s)GD \end{bmatrix} \quad (28)$$

in which, d_f, d_m and d_s represent as fiber, matrix and shear damage coefficient. Also, $D = 1 - (1-d_f)(1-d_m)v_{12}v_{21}$ is damage parameter based on damage coefficients and shear Poisson ratio.

2. Materials and Methods

2.1 Experimental Investigation

The composite used in this study is a multiply composite. Multiply composites are made of different ply placed adjacent to each other, typically consisting of metallic, ceramic, or reinforced polymer ply arranged alternately. The tensile test conducted following ASTM D3039 standards is employed to evaluate the tensile modulus, Poisson's ratio, and tensile strength of five and seven ply Glass/Epoxy composites (**Fig. 1**). This test applies to continuous fiber-reinforced composites, including both unidirectional (UD) and multidirectional (MD) laminates. MD laminates may be composed of single-ply UD laminates, woven fabrics, or other textile fiber structures. Additionally, fiber-reinforced plastic composites (FRP) with discontinuous, randomly oriented reinforcing fibers, such as sheet molding compounds (SMC), can also be assessed using this method (ASTM- D3039, 2008). The standard of D3039ASTM illustrates as following figure schematically.

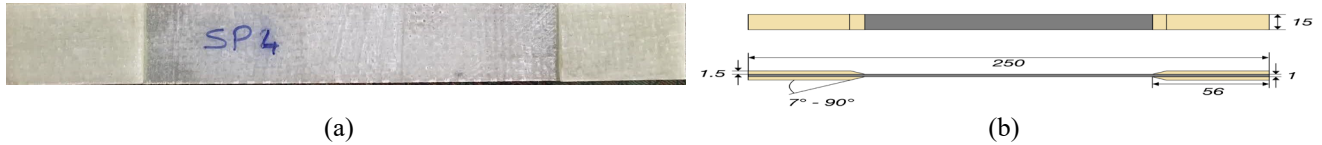


Fig. 1.: (a) and (b), the prepared D3039 specimen for this study and the standard of D3039 ASTM, respectively. Also, the universal test machine is shown in the **Fig. 2**.



Fig. 2. Tensile test machine for the present study.

The aim of conducting the experimental test was to extract the mechanical properties of the composite in order to ensure the accuracy and validity of the simulation results using these data in the software. For this purpose, composite specimens were subjected to tensile testing. The resulting stress-strain curves were obtained and shown in **Fig. 3** and **Fig. 4**.

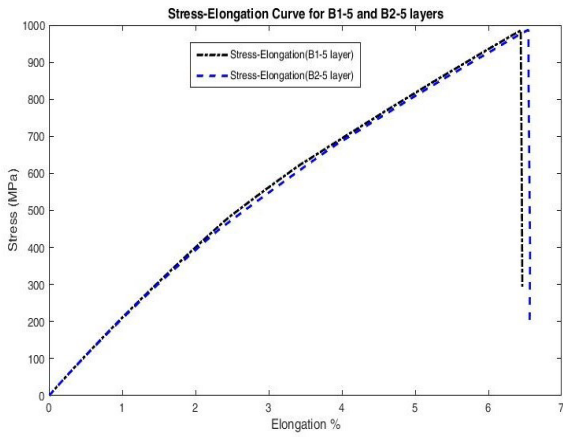


Fig. 3. 5-ply Glass/Epoxy stress-strain experimental diagram.

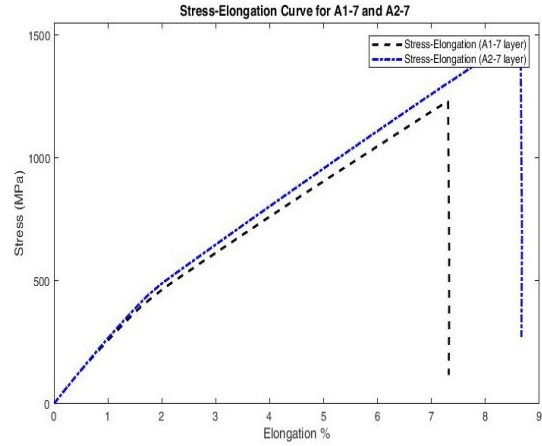


Fig. 4. 7-ply Glass/Epoxy stress-strain experimental diagram.

As observed in the figures, the stress-strain values for the 5-ply glass/epoxy composite are lower than those for the 7-ply glass/epoxy composite. This indicates that the additional ply contribute to enhanced mechanical properties, likely due to increased load-bearing capacity and improved distribution of stress across the composite structure. The properties of the composite’s constituent laminates are presented in the following **Table 1** and **Table 2** for five and seven ply of Glass/Epoxy composites.

Table 1. Mechanical properties of composite ply (5-ply glass /epoxy). The units of E and G are MPa.

G_{13}	G_{23}	G_{12}	ν_{13}	ν_{23}	ν_{12}	E_3	E_2	E_1
8294	8268	8294	0.23	0.24	0.24	0	53850	53580

Furthermore, it was shown that the 7-ply configuration exhibits greater toughness and overall durability compared to the 5-ply variant, suggesting that the plying sequence and density play a crucial role in the composite’s performance under mechanical loading conditions (**Table 2**).

Table 2. Mechanical properties of composite ply (7-ply glass /epoxy)

G_{13}	G_{23}	G_{12}	ν_{13}	ν_{23}	ν_{12}	E_3	E_2	E_1
12050	12060	12050	0.23	0.24	0.24	0	60000	60000

3. Numerical Method

The present study uses a numerical method based on ANSYS programming to prediction of failure in composite materials under tensile loading. The composite structure is built as laminate using pre- and post-processing tools to mimic ply stacking. The processor supports diverse composite types and integrates with ANSYS Workbench, allowing custom modifications in the modeling process. Mechanical loads are applied using ANSYS solver modules. Overall, the simulation workflow combines the custom ANSI C-based processor with the ANSYS environment. The composite modeling procedure involves several steps illustrated schematically in **Fig. 5**. The material used in the proposed laminated composite consists of a transversely isotropic high-strength composite with an orthotropic epoxy matrix reinforced by glass fibers, which is applied in the shell components. It should also be noted that, in the material property definition section, the damage criterion option must be activated to enable damage analysis with in the software. Moreover, all the necessary operations are available in the software’s material library. Using ANSYS software, the results were obtained for both the entire specimen and each individual composite ply, followed by a detailed analysis.

3.1 Numerical Modeling

A numerical simulation was carried out to examine the mechanical behavior of two glass/epoxy composite plates connected by a metal rivet using ANSYS Composite Post-process. The rivet was modeled as the anchoring point, with all degrees of freedom constrained at the rivet to reflect a fixed boundary condition (**Fig. 6**).

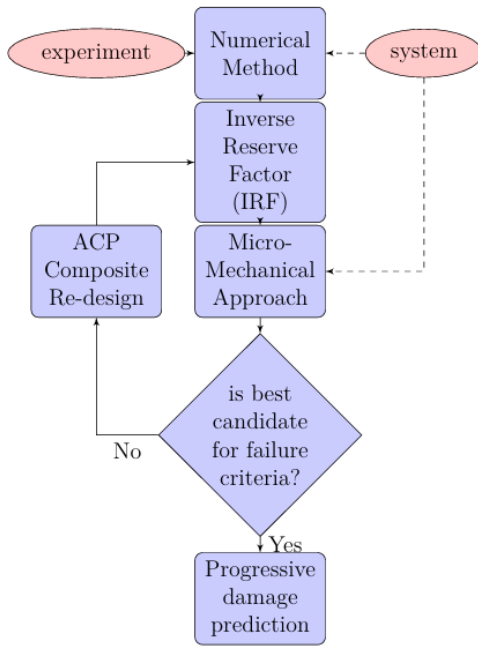


Fig. 5. Composite modeling procedure, schematically.

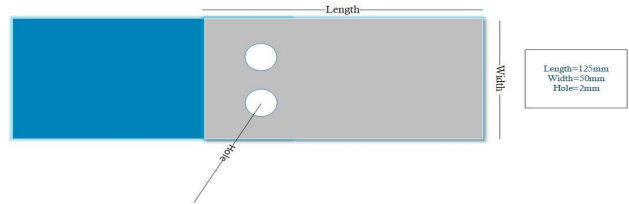


Fig. 6. Glass/Epoxy modeling features, schematically.

On the opposite edge of the assembly, a tensile load was applied to the composite plate, creating a realistic loading scenario for the jointed system. Mesh sensitivity was rigorously analyzed by generating models with varying element sizes, particularly focusing on high mesh density around the rivet hole and the plate contact interface to capture detailed stress variations (Fig. 7).

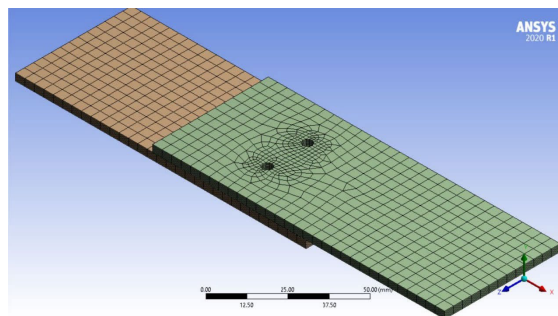


Fig. 7. Meshing on jointed two layer.

This approach enabled a thorough evaluation of how mesh refinement influences the predicted stress distributions and failure zones, all while maintaining a balance between computational efficiency and solution accuracy. The study emphasized the critical nature of both boundary condition application and mesh design in achieving reliable predictions for progressive damage and failure initiation in composite-riveted structures. The numerical modeling was performed in ANSYS, and the results related to progressive damage were extracted. The analysis includes stress, strain, and overall displacement data, along with the failure sequence of each ply. However, this section focuses on the overall analysis results, which are presented in Table 3 and Table 4. In ANSYS software, progressive damage prediction is performed using the Inverse Reserve Factor (IRF). Therefore, it is necessary to provide a brief explanation of this factor before discussing the ply failure results. The IRF represents the ratio of the applied load to the failure load for each ply, evaluated according to the selected damage criterion. When the IRF value exceeds one, failure has occurred; if it is less than one, the material is still intact. The flowchart below illustrates the procedure for computing the Inverse Reserve Factor for the composite material. The central goal of this study is to predict which ply fails 1st and which fails last based on the IRF and the implemented damage criteria in ANSYS. The corresponding modeling and results are presented accordingly.

Table 3. Numerical results of five-ply composite

Effective stress (MPa)	Total displacement (mm)	Total strain
1712.3	1.0926	0.085

Table 4. Numerical results Seven-ply composite

Effective stress (MPa)	Total displacement (mm)	Total strain
2389.9	1.6119	0.28

4. Result and Discussion

In this section, the outcomes derived from various failure criteria were thoroughly analyzed with the objective of accurately predicting the damaged ply within the composite material. To achieve a comprehensive understanding of the failure mechanisms, multiple well-established failure theories were systematically evaluated. These included the HASHIN, Puck, and Hoffman criteria, as well as the maximum stress and maximum strain criteria. By comparing and contrasting these different approaches, the study aimed to provide an inclusive assessment of ply failure prediction, considering both the complex stress states and material responses. This multi-criteria evaluation facilitates a more robust and reliable prediction framework, which is essential for enhancing the design and durability of composite structures.

4.1 Hashin Failure Criterion

The HASHIN failure criterion is widely used for predicting failure in composite materials, particularly unidirectional fiber composites. It distinguishes different failure modes such as fiber tension, fiber compression, matrix tension, and matrix compression, making it effective for composites' ply. The criterion evaluates stress states in each ply and determines the onset of damage based on these modes (**Table 5**). For a better understanding of the above chart, the order of failure, maximum stress, maximum strain, and also the inverse reserve factor based on the HASHIN criterion are expressed in three forms.

Table 5. HASHIN damage criterion for five-layer composite

IRF	Max strain	Max stress	ply failure sequence
15.725	0.067339	1670.7	4th ply of the 1th layer
15.659	0.067065	1668.4	2th ply of the 1th layer
9.0037	0.083353	1701.7	1th ply of the 1th layer
8.6609	0.084	1712.3	5th ply of the 1th layer
8.5588	0.08187	1684.7	3th ply of the 1th layer
0.11025	0.00042704	27.511	5th ply of the 2th layer
0.074175	0.000537749	18.879	1th ply of the 2th layer
0.055517	0.00063249	21.4	4th ply of the 2th layer
0.040001	0.00073385	15.873	2th ply of the 2th layer
0.013805	0.00098107	18.14	3th ply of the 2th layer

As indicated in **Table 5** the HASHIN failure criterion shows that the fourth ply of the first layer (in the five-layer composite) experiences the first ply failure (FPF), whereas the third ply of the same layer fails last (LPF). Similarly, for the second layer, the fifth ply corresponds to the FPF and the third ply represents the LPF. This means that for composites composed of seven layers, the analysis focuses on predicting the order in which each layer will fail, relying on established damage criteria. Maximum strain and stress in **Table 5** to **Table 14** is related to the critical amount of these parameters for ply in each layers. The HASHIN criterion, which considers different failure modes specific to composite materials such as fiber tension, fiber compression, matrix tension, and matrix compression, is employed first to analyze this sequence. This approach provides insight in to progressive damage in multilayer composites, enhancing the prediction of failure modes under mechanical loading. This methodology is crucial for designing layered composites with improved reliability by understanding each layer's vulnerability under stress (**Table 6**).

Table 6. HASHIN damage criterion for seven-ply composite

IRF	Max strain	Max stress	ply failure sequence
22.754	0.29572	2457.9	6th ply of the 1th layer
22.562	0.15695	2431.8	4th ply of the 1th layer
22.06	0.29	2300.4	2th ply of the 1th layer
11.992	0.29575	2369.5	1th ply of the 1th layer
11.779	0.1570	2449.7	7th ply of the 1th layer
11.187	0.16506	2337.9	3th ply of the 1th layer
11.128	0.16409	2291.4	5th ply of the 1th layer
0.13984	0.10441	25.545	1th ply of the 2th layer
0.057806	0.035977	8.107	2th ply of the 2th layer
0.025	0.094109	2.2903	4th ply of the 2th layer
0.01994	0.014066	6.123	3th ply of the 2th layer
0.0184	0.036	2.1448	6th ply of the 2th layer
0.01398	0.0019692	2.4443	7th ply of the 2th layer
0.01214	0.0033544	2.2178	5th ply of the 2th layer

As indicated in **Table 7**, the HASHIN failure criterion shows that the sixth ply of the first layer (in the seven-layer composite) experiences the first ply failure (FPF), whereas the fifth ply of the same layer fails last (LPF). Similarly, for the second layer, the first ply corresponds to the FPF and the fifth ply represents the LPF.

4.2 Hoffman Failure Criterion

The Hoffman failure accounts for the combined influence of normal and shear stresses acting on the material, providing a single criterion for predicting failure under complex loading conditions (Echaabi et al., 1996). It assesses the stress distribution

within each lamina to determine when the material will begin to deteriorate or fail (**Table 7** and **Table 8**). To clarify the results shown in the chart, the progression of failure, along with the maximum stress, maximum strain, and the inverse reserve factor determined from the Hoffman model, are represented in three distinct formats.

Table 7. Hoffman damage criterion for five-ply composite

IRF	Max strain	Max stress	ply failure sequence
15.747	0.067339	1670.7	4th ply of the 1st layer
15.686	0.067065	1668.4	2th ply of the 1st layer
8.812	0.083353	1701.7	1th ply of the 1st layer
8.5665	0.084	1712.3	7th ply of the 1st layer
8.3726	0.08187	1684.7	3th ply of the 1st layer
0.10772	0.00042704	27.511	5th ply of the 2th layer
0.072591	0.000537749	18.879	1th ply of the 2th layer
0.052947	0.00063249	21.4	4th ply of the 2th layer
0.039523	0.00073385	15.873	2th ply of the 2th layer
0.01329	0.00098107	18.14	3th ply of the 2th layer

For the five-layer configuration, the Hoffman damage criterion was employed to evaluate ply-level failure. As summarized in **Table 7**, the results reveal that, according to the Hoffman criterion, the fourth ply within the first laminate layer is the first to fail (FPF), while the third ply in the same layer undergoes failure last (LPF). Similarly, in the second laminate layer, the fifth ply exhibits the initial failure (FPF), whereas the third ply reaches the final failure (LPF).

Table 8. Hoffman damage criterion for seven ply composite

IRF	Max strain	Max stress	ply failure sequence
22.644	0.29572	2457.9	6th ply of the 1st layer
22.484	0.15695	2431.8	4th ply of the 1st layer
22.093	0.29	2300.4	2th ply of the 1st layer
12.129	0.29575	2369.5	1th ply of the 1st layer
11.29	0.1570	2449.7	7th ply of the 1st layer
11.291	0.16506	2337.9	3th ply of the 1st layer
11.234	0.16409	2291.4	5th ply of the 1st layer
0.1347	0.10441	25.545	1th ply of the 2th layer
0.0562	0.035977	8.107	2th ply of the 2th layer
0.024	0.094109	2.2903	4th ply of the 2th layer
0.01887	0.014066	6.123	3th ply of the 2th layer
0.018198	0.036	2.1448	5th ply of the 2th layer
0.01378	0.0019692	2.4443	7th ply of the 2th layer
0.01233	0.0033544	2.2178	1th ply of the 2th layer

For the seven-layer configuration, the Hoffman damage criterion was applied to predict the onset and progression of ply failure. As summarized in **Table 8**, the Hoffman criterion indicates that in the first laminate layer, the sixth ply experiences the first-ply failure (FPF), whereas the third ply of the same layer fails last (LPF). Likewise, within the second layer, the first ply shows the earliest failure (FPF), while the same ply also undergoes the final failure (LPF).

4.3 Maximum Stress Failure Criterion (Ms)

The Maximum Stress theory is a fundamental approach used to assess the structural integrity of composite materials (Li, 2020). It operates on the principle that failure occurs when any stress component—longitudinal, transverse, or shear—surpasses its corresponding material strength limit. Each lamina is evaluated independently, and no interaction between stress components is assumed. This simplicity makes the method suitable for preliminary failure analysis of unidirectional composites under multiaxial loading conditions (**Table 9** and **Table 10**).

Table 9. Maximum stress criterion for five-ply composite

IRF	Max strain	Max stress	ply failure sequence
15.698	0.067339	1670.7	4th ply of the 1st layer
15.634	0.067065	1668.4	2th ply of the 1st layer
0.90025	0.083353	1701.7	1th ply of the 1st layer
8.5721	0.084	1712.3	5th ply of the 1st layer
8.5579	0.08187	1684.7	3th ply of the 1st layer
0.1025	0.00042704	27.511	5th ply of the 2th layer
0.06533	0.000537749	18.879	1th ply of the 2th layer
0.0555	0.00063249	21.4	4th ply of the 2th layer
0.04	0.00073385	15.873	2th ply of the 2th layer
0.01378	0.00098107	18.14	3th ply of the 2th layer

For the five-layer configuration, the MS damage criterion was utilized to forecast the initiation and development of ply failure. According to **Table 9**, the MS criterion reveals that in the first laminate layer, the fourth ply fails first (FPF), whereas

the third ply is the last to failure (LPF). Similarly, in the second layer, the fifth ply experiences the earliest failure (FPF), and the third ply undergoes the final failure (LPF).

Table 10. Maximum stress damage criterion for seven ply composite

IRF	Max strain	Max stress	ply failure sequence
22.673	0.29572	2457.9	6th ply of the 1th layer
22.484	0.15695	2431.8	4th ply of the 1th layer
21.97	0.29	2300.4	2th ply of the 1th layer
11.722	0.29575	2369.5	1th ply of the 1th layer
11.512	0.1570	2449.7	7th ply of the 1th layer
10.964	0.16506	2337.9	3th ply of the 1th layer
11.917	0.16409	2291.4	5th ply of the 1th layer
0.1221	0.10441	25.545	1th ply of the 2th layer
0.05779	0.035977	8.107	2th ply of the 2th layer
0.0243	0.094109	2.2903	4th ply of the 2th layer
0.0198	0.014066	6.123	3th ply of the 2th layer
0.018347	0.036	2.1448	6th ply of the 2th layer
0.01596	0.0019692	2.4443	7th ply of the 2th layer
0.01233	0.0033544	2.2178	5th ply of the 2th layer

For the seven-layer configuration, the MS damage criterion was employed to analyze the initiation and evolution of ply failure. Based on the results presented in Table 10, the MS criterion identifies the sixth ply in the first laminate layer as the first to fail (FPF), while the third ply of the same layer experiences the final failure (LPF). Similarly, in the second layer, the first ply exhibits the earliest failure (FPF), and the fifth ply reaches failure last (LPF).

4.4 Maximum Strain Failure Criterion

The Maximum Strain criterion serves as a fundamental analytical approach for predicting failure in composite laminates. This model postulates that failure occurs when any principal or shear strain component within a lamina exceeds its corresponding allowable limit (Echaabi et al., 1996; Li, 2020). Each ply is evaluated independently, and the criterion assumes no interaction among the different strain components. Owing to its simplicity and direct correlation with measurable deformation parameters, the Maximum Strain theory is often employed for preliminary evaluations of composite failure under complex loading conditions (Table 11, Table 12). In the presented chart, the outcomes are organized to highlight the sequence of failure initiation, the maximum strain and stress values recorded prior to failure, and the inverse reserve factor as determined through the Maximum Strain formulation. In the fifth-layer configuration, the maximum strain criterion was used to predict the initiation and progression of ply failure. As shown in Table 11, the criterion identifies the fourth ply in the first laminate layer as the earliest to fail (FPF), while the third ply of that layer fails last (LPF). Similarly, in the second layer, the fifth ply is the first to experience failure (FPF), and the third ply is the last to fail (LPF). This approach effectively captures the sequence of damage evolution within the composite laminate’s layers. Also, for seven-layer FPF and LPF are obtained as follows:

Table 11. Maximum strain criterion for five ply composite.

IRF	Max strain	Max stress	ply failure sequence
13.33	0.067339	1670.7	4th ply of the 1th layer
28.13	0.067065	1668.4	2th ply of the 1th layer
8.555	0.083353	1701.7	1th ply of the 1th layer
8.6	0.084	1712.3	5th ply of the 1th layer
8.3527	0.08187	1684.7	3th ply of the 1th layer
0.05	0.00042704	27.511	5th ply of the 2th layer
0.03322	0.000537749	18.879	1th ply of the 2th layer
0.026185	0.00063249	21.4	4th ply of the 2th layer
0.02268	0.00073385	15.873	2th ply of the 2th layer
0.010452	0.00098107	18.14	3th ply of the 2th layer

Table 12. Maximum strain criterion for seven layer composite

IRF	Max strain	Max stress	ply failure sequence
19.066	0.29572	2457.9	6th ply of the 1th layer
18.97	0.15695	2431.8	4th ply of the 1th layer
18.75	0.29	2300.4	2th ply of the 1th layer
15.5	0.29575	2369.5	1th ply of the 1th layer
15.338	0.1570	2449.7	7th ply of the 1th layer
14.663	0.16506	2337.9	3th ply of the 1th layer
14.601	0.16409	2291.4	5th ply of the 1th layer
0.13984	0.10441	25.545	1th ply of the 2th layer
0.03431	0.035977	8.107	2th ply of the 2th layer
0.0135	0.094109	2.2903	4th ply of the 2th layer
0.0198	0.014066	6.123	3th ply of the 2th layer
0.0105	0.036	2.1448	6th ply of the 2th layer
0.0048	0.0019692	2.4443	7th ply of the 2th layer
0.003	0.0033544	2.2178	5th ply of the 2th layer

In the seven-layer configuration, the maximum strain criterion was applied to evaluate the initiation and progression of ply failure. As presented in Table 12, the analysis indicates that the sixth ply within the first laminate layer experiences the first-ply failure (FPF), while the fifth ply of that same layer is the last to fail (LPF). Similarly, in the second layer, the first ply undergoes both the earliest and final failure events for fifth layer (FPF and LPF, respectively).

4.4.1 Puck Failure Criterion

The Puck failure theory provides a detailed framework for assessing damage initiation and progression in fiber-reinforced composites (Echaabi et al., 1996). It focuses on evaluating the stresses acting within each lamina to identify potential fracture surfaces, distinguishing clearly between fiber breakage and inter-fiber (matrix) failure. This criterion allows for an accurate prediction of composite behavior under multidirectional stress states (**Table 13** and **Table 14**). For clarity, the graphical results include the sequence of failure events, the peak stress and strain responses, and the inverse reserve factor as derived from the Puck formulation, presented in three distinct formats.

Table 13. Puck damage criterion for five ply composite

IRF	Max strain	Max stress	ply failure sequence
15.748	0.067339	1670.7	4th ply of the 1th layer
15.681	0.067065	1668.4	2th ply of the 1th layer
9.056	0.083353	1701.7	1th ply of the 1th layer
9.017	0.084	1712.3	5th ply of the 1th layer
8.9064	0.08187	1684.7	3th ply of the 1th layer
0.1167	0.00042704	27.511	5th ply of the 2th layer
0.08	0.000537749	18.879	1th ply of the 2th layer
0.055528	0.00063249	21.4	4th ply of the 2th layer
0.04001	0.00073385	15.873	2th ply of the 2th layer
0.013824	0.00098107	18.14	3th ply of the 2th layer

In the fifth-layer configuration, the Puck criterion was applied to predict the initiation and evolution of ply failure. As shown in **Table 14**, the analysis reveals that the sixth ply in the first laminate layer undergoes the first-ply failure (FPF), while the fifth ply of that same layer fails last (LPF). Likewise, in the second layer, the first and fifth ply exhibits both the earliest and final failure events (FPF and LPF, respectively).

Table 14. Puck criterion for seven ply composite

IRF	Max strain	Max stress	ply failure sequence
22.826	0.29572	2457.9	6th ply of the 1th layer
22.633	0.15695	2431.8	4th ply of the 1th layer
22.103	0.29	2300.4	2th ply of the 1th layer
12.985	0.29575	2369.5	1th ply of the 1th layer
12.758	0.1570	2449.7	7th ply of the 1th layer
12.069	0.16506	2337.9	3th ply of the 1th layer
11.988	0.16409	2291.4	5th ply of the 1th layer
0.1513	0.10441	25.545	1th ply of the 2th layer
0.0580	0.035977	8.107	2th ply of the 2th layer
0.025	0.094109	2.2903	4th ply of the 2th layer
0.02	0.014066	6.123	3th ply of the 2th layer
0.01856	0.036	2.1448	6th ply of the 2th layer
0.01596	0.0019692	2.4443	7th ply of the 2th layer
0.01233	0.0033544	2.2178	5th ply of the 2th layer

Based on all the evaluated criteria, it can be concluded that the different failure models consistently and accurately predict the sequential failure of laminate layers. The results demonstrate a strong agreement among the criteria, confirming their reliability in identifying the order of layer failure. Furthermore, the failure patterns for all layers were systematically arranged and compared across the applied criteria, with the corresponding findings illustrated in the following figures (**Fig. 8** and **Fig. 9**).

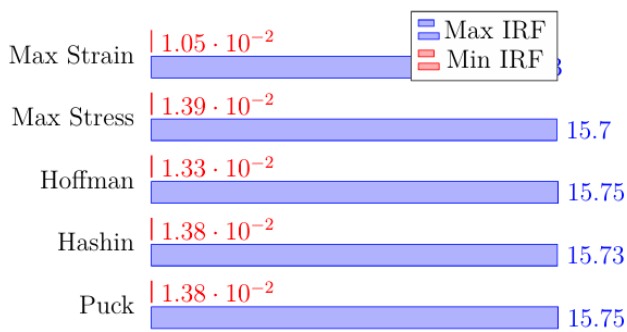


Fig. 8. FPF prediction for the five-layer Glass/Epoxy based on different criteria

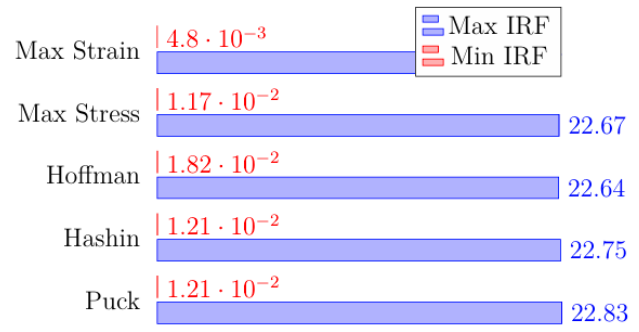


Fig. 9. FPF prediction for the seven-layer Glass/Epoxy based on different criteria

It is evident that, for the five-layer composite, the Puck and HASHIN criteria yield the highest stress magnitudes and probabilities of failure, whereas the maximum strain criterion predicts the lowest failure tendency among all evaluated models.

It can be observed that, for the seven-layer composite, the Puck and HASHIN criteria predict the highest stress values and failure probabilities, whereas the maximum strain criterion indicates comparatively lower failure potential among all evaluated criteria. Based on recent studies, the Puck and HASHIN failure criteria demonstrate high predictive accuracy for composite damage analysis, particularly in aerospace-grade laminates. The Puck criterion achieves an accuracy rate of approximately 90–95% for matrix-dominated and inter-fiber failures, due to its precise differentiation between failure modes and its empirical calibration against experimental data. Similarly, the HASHIN criterion shows an average accuracy of 85–92%, especially effective in fiber-dominated fracture prediction under tensile and compressive loads.

5. Conclusion

The assessment of damage initiation and propagation in composite structures remains a key factor in advancing the reliability of aerospace materials. Accurate prediction of progressive damage in individual plies ensures structural integrity, service life, and operational safety. In this study, numerical and analytical approaches were employed to characterize damage evolution under quasi-static loading, including tensile conditions, in bolted composite configurations. The comparative evaluation of several failure criteria revealed that the Puck and HASHIN models exhibited the highest predicted damage indices and failure probabilities for both five-layer and seven-layer laminates, while the maximum strain criterion consistently produced the lowest predictions. These outcomes highlight the superior sensitivity of the Puck and HASHIN criteria in identifying potential failure zones and capturing both matrix- and fiber-dominated damage modes. The Puck criterion achieves an accuracy rate of approximately 90–95% for matrix-dominated and inter-fiber failures, and the HASHIN criterion shows an average accuracy of 85–92%, especially effective in fiber-dominated fracture prediction under tensile and compressive loads. Consequently, these two models are recommended for use in the accurate numerical assessment of durability and for developing efficient design methodologies that enhance the structural performance and longevity of aerospace composite components.

References

- ASTM (2008), American Society for Testing and Materials. ASTM 3039/D3039M. Standard Test Method for Tensile Properties of Polymer Matrix Composites Materials. Pennsylvania, USA: ASTM.
- Bogdanovich, A. (2009). *Progressive failure modeling and strength predictions of 3D woven composites*. Paper presented at the 50th AIAA/ASME/ASCE/AHS/ASC Structures, Structural Dynamics, and Materials Conference 17th AIAA/ASME/AHS Adaptive Structures Conference 11th AIAA No.
- Chang, F.-K., & Chang, K.-Y. (1987). A progressive damage model for laminated composites containing stress concentrations. *Journal of Composite Materials*, 21(9), 834–855.
- Christensen, R. (1997). Stress based yield/failure criteria for fiber composites. *International journal of solids and structures*, 34(5), 529–543.
- Cutting, R. A. (2025). An evaluation of progressive damage analysis methods for modeling low velocity impact of thermoplastic composites. *Journal of Composite Materials*, 59(3), 395–416.
- Dano, M.-L., Gendron, G., & Picard, A. (2000). Stress and failure analysis of mechanically fastened joints in composite laminates. *Composite structures*, 50(3), 287–296.
- Echaabi, J., Trochu, F., & Gauvin, R. (1996). Review of failure criteria of fibrous composite materials. *Polymer composites*, 17(6), 786–798.
- Ghosh, G., Biswas, D., & Bhattacharyya, R. (2025). Advancements in multiscale modeling of damage in composite materials: A comprehensive review. *Composites Part B: Engineering*, 112819.
- Gljušić, M., Franulović, M., Žužek, B., & Žerovnik, A. (2022). Experimental validation of progressive damage modeling in additively manufactured continuous fiber composites. *Composite structures*, 295, 115869.
- Harris, C. E., Coats, T., Allen, D. H., & Lo, D. C. (1997). A progressive damage model and analysis methodology for predicting the residual strength of composite laminates. *Composites Technology and Research*, 19(1), 3–9.
- Hashin, Z. (1980). *Fatigue Failure Criteria for Unidirectional Fiber Composites*. Retrieved from
- Hashin, Z., & Rotem, A. (1973). A fatigue failure criterion for fiber reinforced materials. *Journal of Composite Materials*, 7(4), 448–464.
- Kaleel, I., Petrolo, M., Waas, A., & Carrera, E. (2018). Micromechanical progressive failure analysis of fiber-reinforced composite using refined beam models. *Journal of Applied Mechanics*, 85(2), 021004.
- Khansari, N. M., Fakoor, M., & Berto, F. (2019). Probabilistic micromechanical damage model for mixed mode I/II fracture investigation of composite materials. *Theoretical and Applied Fracture Mechanics*, 99, 177–193.
- Kodagali, K. (2017). Progressive failure analysis of composite materials using the Puck failure criteria.
- Li, S. (2020). The maximum stress failure criterion and the maximum strain failure criterion: their unification and rationalization. *Journal of Composites Science*, 4(4), 157.
- Lin, S., Yang, L., Xu, H., Jia, X., Yang, X., & Zu, L. (2021). Progressive damage analysis for multiscale modelling of composite pressure vessels based on Puck failure criterion. *Composite structures*, 255, 113046.

- Mehri Khansari, N., & Aliha, M. (2023). Mixed-modes (I/III) fracture of aluminum foam based on micromechanics of damage. *International Journal of Damage Mechanics*, 32(4), 519–548.
- Mehri Khansari, N., Danandeh Hesar, H., & Zare Hosseinabadi, S. (2024). Orthotropic failure criteria based on machine learning and micro-mechanical matrix adapting coefficient. *Mechanics Based Design of Structures and Machines*, 52(12), 9923–9946.
- Mehri Khansari, N., Ghoreishi, S. M. N., & Al-Rumaithi, A. (2022). Effective Constant of Porous Materials Using Micro-Meso Damage Modeling. *Challenges in Nano and Micro Scale Science and Technology*, 10(2), 43–55.
- Papanikos, P., Tserpes, K., & Pantelakis, S. (2003). Modelling of fatigue damage progression and life of CFRP laminates. *Fatigue & Fracture of Engineering Materials & Structures*, 26(1), 37–47.
- Roy, S., & Srivastav, A. (2017). Multiscale modeling of progressive failure in polymer nanocomposites using nanoscale informed damage mechanics. *Mechanics of Advanced Materials and Structures*, 24(1), 45–63.
- Shamsirband, S., & Mehri Khansari, N. (2021). Micro-mechanical damage diagnosis methodologies based on machine learning and deep learning models. *Journal of Zhejiang University-SCIENCE A*, 22(8), 585–608.
- Shokrieh, M. M., & Omid, M. J. (2010). Dynamic progressive damage modeling of fiber-reinforced composites under different strain rates. *Journal of Composite Materials*, 44(23), 2723–2745.
- Sun, Q., Zhou, G., Meng, Z., Guo, H., Chen, Z., Liu, H., . . . Su, X. (2019). Failure criteria of unidirectional carbon fiber reinforced polymer composites informed by a computational micromechanics model. *Composites Science and Technology*, 172, 81–95.
- Talreja, R. (2006). Multi-scale modeling in damage mechanics of composite materials. *Journal of materials science*, 41(20), 6800–6812.
- Tsai, S. W., & Wu, E. M. (1971). A general theory of strength for anisotropic materials. *Journal of Composite Materials*, 5(1), 58–80.
- Zhang, C., Li, N., Wang, W., Binienda, W. K., & Fang, H. (2015). Progressive damage simulation of triaxially braided composite using a 3D meso-scale finite element model. *Composite structures*, 125, 104–116.
- Zheng, T., Guo, L., Ding, J., & Li, Z. (2022). An innovative micromechanics-based multiscale damage model of 3D woven composites incorporating probabilistic fiber strength distribution. *Composite structures*, 287, 115345.



© 2026 by the authors; licensee Growing Science, Canada. This is an open access article distributed under the terms and conditions of the Creative Commons Attribution (CC-BY) license (<http://creativecommons.org/licenses/by/4.0/>).